CORROSION SCIENCE AND TECHNOLOGY, Vol.24, No.2(2025), pp.51~62 pISSN 1598-6462 / eISSN 2288-6524
[Research Paper] DOI: https://doi.org/10.14773/cst.2025.24.2.51

Improvement of Corrosion Resistance of Stainless Steel 316 by Electroless Phosphorus Nickel-Titania Composite Coating

Nabaa S. Radhi[1], Farah Sami Rasheed[2], Zainab Al-Khafaji[3,4,†], Kulthoom Obaid Ali[1], and Rasha Ghazi[1]

[1]*Metallurgical Engineering Department, College of Material Engineering, University of Babylon, Babylon, Iraq*
[2] *Ministry of Education, Babylon, Iraq*
[3]*Department of Civil Engineering, Faculty of Engineering and Built Environment, Universiti Kebangsaan Malaysia, 43600 UKM Bangi, Selangor, Malaysia*
[4]*Imam Ja'afar Al-Sadiq University; Qahira, Baghdad, Iraq*
(Received May 07, 2024; Revised December 06, 2024; Accepted December 09, 2024)

To enhance the functional performance of steel components in industrial and consumer applications, it is essential to address challenges such as corrosion susceptibility, environmental toxicity, and surface aesthetics. Consequently, electroless nickel-phosphorus (Ni-P) coatings on 316 stainless steel substrates have gained considerable attention. This study explores the deposition of low-phosphorus Ni-P coatings incorporated with titania (TiO_2) particles, with sizes ranging from 10 to 30 μm. Coating solutions were formulated with TiO_2 concentrations of 0, 5, and 10 g/L, and deposition durations were set at 30 and 60 minutes. The coated samples were systematically evaluated using coating thickness measurements, surface roughness analysis, Vickers hardness testing, energy dispersive spectroscopy (EDS), scanning electron microscopy (SEM), and potentiodynamic polarization testing in 3.5% NaCl solution. Results revealed that the inclusion of TiO_2 particles significantly enhanced the mechanical performance of the coatings, as evidenced by increased hardness values compared to both the bare substrate and TiO_2-free Ni-P coatings. Additionally, electrochemical analysis indicated a marked improvement in corrosion resistance, with the TiO_2-reinforced coating achieving a 74% reduction in corrosion rate relative to the uncoated steel. These findings suggest that TiO_2-doped electroless Ni-P coatings are a promising solution for advanced surface engineering applications.

Keywords: *Electroless, Nickel-phosphor, Titania particles, Composite nickel coating*

1. Introduction

Pipelines are an essential component of the gas and oil transport infrastructure. Pipelines are widely acknowledged as Canada's optimal and economically efficient method for transporting substantial quantities of petrol products. Gas and oil are efficiently conveyed through pipelines, facilitating seamless transportation from excavation sites to terminals, refineries, and markets [1–4]. Pipeline erosion/corrosion damage poses a growing concern within the petroleum industry, primarily due to the internal pipeline environment's highly corrosive nature. Carbon dioxide (CO_2) gas within pipelines induces internal corrosion [5,6].

In contrast, the interaction between the internal surface of the pipeline and solid particles transported in the oil leads to a gradual mechanical degradation of the material [7–9]; the combined impact of corrosion and erosion results in significant material degradation within the pipeline. In conjunction with erosion/corrosion degradation, dents, and gauges significantly exacerbate pipeline failure likelihood [10]. Numerous methodologies have been postulated for safeguarding pipelines against potential impairment, wherein internal coatings have emerged as the preeminent technique [11].

Pipeline corrosion refers to the degradation of pipe material and its associated system since its interaction with the operational environment [12,13]. It influences pipelines and associated components composed of metallic and non-metallic materials [14]. The issue of pipeline corrosion and its consequential catastrophic failures incurs significant economic losses amounting to

†Corresponding author: p123005@siswa.ukm.edu.my

billions of dollars. The predicted total annual cost of corrosion in America in 2016, encompassing both direct and indirect expenses, surpassed USD 1.1 trillion [15,16].

Corrosion poses a significant challenge, to put it succinctly. It primarily impacts metallic pipelines, including but not limited to stainless steel, carbon steel, copper, cast iron, aluminum, and alloy steel pipes, commonly employed in submerged, underground, buried, or similar pipeline applications [17,18]. Designing and selecting optimal systems and materials for pipelines and their corrosion protection systems is critically significant in the oil and gas industry [19,20]. By federal regulations, pipelines deemed high-risk for transporting oil, gas, or other hazardous substances must adhere to the utilization of dependable and efficient pipe materials and coatings, alongside the implementation of cathodic protection measures [21]. In this analysis, we shall examine the primary forms of corrosion that impact pipelines and the methodologies employed to safeguard this vital infrastructure [22].

When subjected to corrosive agents, pipeline corrosion manifests in both the internal and external surfaces of pipes and associated structures. A multitude of corrosion phenomena can manifest within pipelines [23]. The responses to the substances conveyed through pipelines and external circumstances such as weather collectively contribute. The untreated condition can lead to a costly issue that requires rectification. Pipelines are subject to various forms of corrosion, with certain types being more prevalent than others. These corrosion mechanisms encompass crevice, galvanic, uniform, pitting, and microbiologically affected corrosion. Corrosion may manifest in non-metallic conduits like plastic or carbon fiber materials.

Electroless and electroplating techniques and combining composite materials offer a viable approach in materials engineering for achieving desired surface characteristics such as enhanced corrosion resistance, abrasion resistance, wear resistance, and hardness [24–27]. These coatings' production involves co-deposing different second-phase particles into an alloy matrix or metal through electroless or electrodeposited methods. The process of co-depositing can be accomplished using a wide range of suspended particulates that do not exhibit any significant interaction with the plating bath. Electroless nickel coatings are a promising solution to address the constraints [28]. These coatings are derived from traditional binary Ni–Pb films and have been widely utilized in various biomedical applications, including implant coatings, medical device coatings, and drug delivery systems [29]. The remarkable performance of these entities can be attributed to their exceptional adhesion properties across diverse substrates, shapes, and dimensions, as well as their elevated hardness in the annealed condition, which is primarily achieved by forming nickel phosphides, which enhance corrosion and wear resistance [30,31]. In the past few decades, there has been a significant focus on advancing the electroless deposition of nickel-based coatings in the biomedical field, which has been motivated by the increasing demand for enhanced metallic materials' surface features, allowing them to be utilized in more challenging and demanding biomedical environments. Composite bioactive, quaternary, and ternary coatings were developed for biomedical applications [32,33]. The biomedical application involved the evaluation of the co-deposition of diverse inorganic particles for the electroless plating of a Ni-Pb composite coating. These particles included SiO_2, SiC, TiO_2, ZrO_2, and B_4C [34–36].

Antar et al. developed Ni–B–TiO_2 composite coatings [37], incorporating TiO_2 sol into the bath solution throughout the preparation process. A comprehensive investigation was undertaken to achieve the desired goal, encompassing various tests, including multi-pass scratch testing, reciprocating sliding testing, progressive load scratch testing, microhardness testing, XRD, and SEM. Based on the observations, it can be concluded that the Ni-B matrix experienced notable modifications in its microstructure due to the inclusion of TiO_2 structures, whether crystalline or amorphous. Due to its dense microstructure, the Ni-B deposit demonstrated enhanced scratch response and superior wear resistance, which is attributed to this material's utilization. The investigation conducted by Ashassi-Sorkhabi and Rafizadeh [38] aimed to analyze the impact of coating duration and thermal treatment on the corrosion characteristics of electroless Ni-Pb deposited on mild steel samples, which were subsequently subjected to a 3.50% NaCl solution. The findings of their investigation demonstrated that the duration of heat treatment and coating application significantly influenced corrosion behaviors. The experimental findings

have exhibited that prolonging the electroless Ni-Pb coating application on mild steel specimens significantly decreases the corrosion rate detected in said specimens.

Recent investigations have extensively analyzed the corrosion behavior of electroless nickel-phosphorus (Ni-P) composite coatings, with a particular focus on the incorporation of reinforcement particles such as titanium dioxide (TiO_2) to enhance corrosion resistance in aggressive environments, including seawater [39]. The inclusion of TiO_2 within the Ni-P matrix has demonstrated a marked improvement in corrosion resistance by refining the coating's microstructure and facilitating the formation of a denser and more homogeneous protective layer . The corrosion resistance of Ni-P coatings is substantially influenced by phosphorus content, with higher levels typically correlating with enhanced protective properties. However, the incorporation of additional alloying elements and particulate reinforcements, such as TiO_2, further amplifies this resistance by altering the coating's microstructure and enhancing its electrochemical performance [40]. In the oil and gas sector, where pipelines are subjected to severe erosive and corrosive conditions, electroless Ni-P composite coatings have been shown to effectively mitigate material degradation. For instance, the inclusion of ductile reinforcements such as nickel-titanium (NiTi) particles into the Ni-P matrix significantly improves both erosion and corrosion resistance, thereby extending the operational lifespan of pipeline systems [41]. Furthermore, recent studies on the co-deposition of graphene oxide (GO) and TiO_2 into the Ni-P matrix have revealed superior corrosion and tribological performance. These advancements are attributed to the synergistic interactions between GO's exceptional electrochemical properties and TiO_2's ceramic characteristics, which together enhance the structural integrity and protective capabilities of the coatings [42]. This investigation aims to evaluate the corrosion behavior of stainless steel pipelines protected by electroless composite coatings. Specifically, the study will apply Ni-Pb and Ni-Pb-TiO_2 coatings using varying deposition times of 30 and 60 minutes. Titania (TiO_2) will be incorporated into a nickel-phosphor matrix at concentrations of 0%, 0.5%, and 1% by weight to create sacrificial composite coatings. The primary objective is to enhance the corrosion resistance of these coatings in seawater environments, ensuring improved durability and cost-effectiveness for oil pipeline protection.

2. Materials And Methods

The samples employed in all the tests were fabricated utilizing cylindrical molds, resulting in disc-shaped final samples characterized by a thickness of 5mm and a diameter of 10 mm. The measured surface areas of these samples amount to 3.14 cm^2. The sample surface underwent a preparation process starting with grinding using silicon carbide papers in grades ranging from 220 to 1200. After grinding, the surface was meticulously cleaned with distilled water to remove any impurities before electroplating.

For the electrodeposition process, the sample was rinsed with cold water and then immersed in a hydrochloric acid solution (20% concentration) at 21 - 27 ºC for one minute. Another cold rinse followed. The sample was then subjected to anodic etching in a Wood's nickel-strike bath containing $NiCl_2$ and HCl at 43 ºC with a current density of 0.0538 A/cm^2 for 20 seconds. Finally, the sample was immersed in a bath at 43 ºC with the same current density for two minutes and given a final cold rinse.

2.1 Preparation of Substrate and Coating Deposition

The electroless deposition technique applied the Ni-Pb coating to stainless steel 316 specimens (10 mm diameter, 5 mm thick). Substrate preparation involved cleaning with a 10% NaOH solution, followed by acetone reduction and pickling in 30% HCl to remove surface impurities. After rinsing with deionized water, the specimens were activated in a 55 ºC palladium chloride solution for rapid deposition and strong adhesion.

The electroless bath, detailed in Table 1, was maintained at 90±1 ºC, with deposition times of 30 or 60 minutes. Titania was added at concentrations of 0, 0.5, and 1 g/L (Table 2), and the pH was adjusted to 5 using NaOH. Stirring at 300 rpm ensured uniform deposition. Post-deposition, the specimens underwent thermal treatment at 350 ºC for one hour in a vacuum furnace, followed by gradual cooling.

2.2 Tests

The current investigation performed the methodology for the forthcoming experiments to assess the coating

Table 1. Operation conditions and bath composition of the baths utilized [43]

Bath composition and operating conditions	
Nickel sulfate (g/L)	30
Sodium hypophosphite (g/L)	25
Sodium citrate (g/L)	20
Thiourea (mg/L)	2
Temp (degree centigrade)	90±1
pH	5
Coating duration (sec.)	3600
Titania (g/L)	0, 5 and 10

Table 2. The sample description

Sample ID	Description
SN1	316 st.st-Uncoated Sample
SN2	Ni-Pb 30min
SN3	Ni-Pb 60min
SN4	Ni-Pb- 0.5TiO_2, 30min.
SN5	Ni-Pb- 0.5TiO_2, 60min.
SN6	Ni-Pb-1.0TiO_2,30min.
SN7	Ni-Pb-1.0TiO_2,60min

layers' performance; all the tests were conducted at the University of Babylon.

2.2.1 Coating Thickness Measurements

The experimental protocol employs a coating thickness gauge (TT 260). The device demonstrates a precision level with a tolerance of ± 0.1 µm. Measurements were performed at three discrete locations to acquire an average magnitude for the thickness of the sample. The experimental procedure entailed the application of a coating solution comprising Ni-Pb and Ni-Pb-TiO_2, wherein titania was incorporated at amounts of 5 and 10 g/L. The coating procedure was 60 minutes, during which it was executed on stainless steel specimens.

2.2.2 Surface Roughness Test

The surface roughness evaluation was conducted on stainless steel samples coated with Ni-Pb and Ni-Pb-TiO_2 layers, wherein the amount of titania was 5 and 10 g/L, respectively. The duration of the coating process was 60 minutes. The surface roughness evaluation was performed utilizing the TR-100 surface roughness tester. The instrument moves across the specimens' surface to measure and evaluate the level of surface roughness. Featuring a highly sensitive sensor, the apparatus effectively measures and documents the surface roughness of the sample. The obtained data is promptly displayed on the device's screen, ensuring real-time monitoring. The apparatus demonstrates a precision level with a tolerance of ± 0.01 µm.

2.2.3 Hardness test

Ni-Pb and Ni-Pb-TiO_2 coatings were incorporated into titania at 5 and 10 g/L, respectively. The coating procedure entailed depositing multiple layers onto stainless-steel samples and uncoated substrates. The load applied throughout the hardness measurement was 50 g, lasting 10 seconds.

2.2.4 Scanning Electron Microscopy Test (SEM)

The surface deposit layer on the steel specimen, particularly the Ni-Pb and Ni-Pb-TiO_2 layers, was observed using a scanning electron microscopy instrument (Inspect S50, FEI company). Titania, a mate1rial of (5 and 10) g/L, was incorporated into the layers during the 60-minute coating process.

2.2.5 Energy dispersive X-ray (EDX) spectroscopy

The EDX model, specifically the Inspect S50 FEI company model, was employed as an analytical method to ascertain the elemental composition percentages of each layer of a coated specimen. The coating in question consisted of layers of Ni-Pb and Ni-Pb-TiO_2, with the addition of titania at (5 and 10) g/L, respectively. The coating process took 60 minutes and was applied onto stainless steel.

2.2.6 Corrosion test

2.2.6.1 Open Circuit Potential (O.C.P.)

The open circuit potential (O.C.P.), or the equilibrium potential represents the potential condition where the cell does not receive any active current supply. The technique under consideration is a valuable approach to determine the potential difference between the operational and reference electrodes. The (O.C.P), which refers to the voltage versus time data, was meticulously recorded at 5-minute intervals for each specimen. The samples comprised steel and stainless-steel substrates, which were

subsequently coated with a layer of Ni-Pb and Ni-Pb-TiO_2. The titania was added at amounts of (5 and 10) g/L. The durability of the coating was observed for 60 minutes, during which the specimens had been subjected to immersion in a salt solution containing an amount of 3.5%. Sodium chloride (NaCl) is frequently utilized as a corrosion mitigation agent in various applications within the field of materials engineering.

2.2.6.2 Liner Polarization Test

The linear polarization test was meticulously prepared per the standardized procedure outlined in ASTMG5-94 [44]. The Potentiodynamic polarization test, precisely the Mlab Sci-Electwchemica type, was employed to conduct this experiment. The test was conducted in a salt solution, and the samples used were uncoated 316 stainless steel and steel coated with Ni-Pb and Ni-Pb-TiO_2 layers. The titania concentration in the coating was varied at (5 and 10) g/L. The coating lasted 60 minutes, and the specimens were maintained at 30 degrees centigrade. Potentiodynamic polarization experiments have been performed within a three-electrode cell housing an electrolyte salt solution. The working electrode's potential is monitored in relation to a Saturated Calomel electrode (SCE). Between the working electrode and the reference electrode is a voltmeter that is saturated. The rate of corrosion assessment was obtained by implementing the subsequent formula [45].

$$\text{The rate of corrosion (mpy)} = 0.1288\ i_{corr.}\ (E.W.)/A.\rho \quad (1)$$

Where:

E. W. = equivalent weight (g/eq.)

A = area (cm^2)

ρ = density (g/ cm^3)

0.1288 = conversion parameter for time and metric.

$i_{corr.}$ = The current density ($\mu A/cm^2$).

The enhancement percentage was determined for the coated specimens utilizing the subsequent formula [45]:

$$\text{Enhancement percentage} = \left(\frac{CR_0 - CR}{CR_0}\right) \times 100 \quad (2)$$

Whereas:

CR_0 = the corrosion rate of the master specimen (uncoating).

CR = the corrosion rate of the coated specimen (with Ni-Pb and Ni-Pb-TiO_2 layer).

3. Results And Discussion

3.1 Thickness Results

The coating specimens demonstrate 60.8 and 78.8 micrometers thicknesses for the Ni-Pb 60-minute treatment and the Ni-Pb-TiO_2 60-minute treatment, respectively, with titania concentrations of 0.5 and 1.0 weight percent. The experimental findings indicate a direct correlation between the duration of coating and the deposit rates of the (Ni-Pb) coating layers. Additionally, the increase in the added titania percentage also causes an increase in the deposit rates. The observed phenomenon can be ascribed to the significant magnitude of the deposited layer resulting from the electroless solution's interaction with the sample for 60 minutes, specifically when utilizing Ni-Pb-1.0TiO_2.

The findings suggest that the deposition rates of the final coating layers exhibit significant variation. The observed phenomenon can be ascribed to the elevated diffusivity of the species, which arises from TiO_2. Nevertheless, as the quantity of TiO_2 particles escalates, the thickness rate also experiences a corresponding escalation, as evidenced by the data in Fig. 1. Based on the data illustrated in Fig. 1, it is evident that the coating thickness experiences a proportional increase in both the coating time and the percentage of titania (TiO_2) added to the electroless coating solution of nickel. This phenomenon results in the forming of a composite layer of nickel impregnated with (TiO_2) on the surface of the steel sample.

3.2 Surface roughness

Fig. 3 illustrates the results obtained from the analysis of surface roughness performed on the composite coating's surface. Based on the available data, using 0.5 wt% TiO_2 improved the surface smoothness. In the subsequent stages, with the gradual increase in the titania content within the coating solution, the surface roughness exhibited a progressive escalation, ultimately reaching its peak roughness at a concentration of 1.0 weight percent of TiO_2. According to the findings derived from the coating thickness analysis, it is evident that there exists a

direct relationship between the coating thickness and surface roughness, as they both increase proportionally with the augmentation of the TiO_2 content incorporated within the nickel composite layer deposited onto the surface of the steel sample.

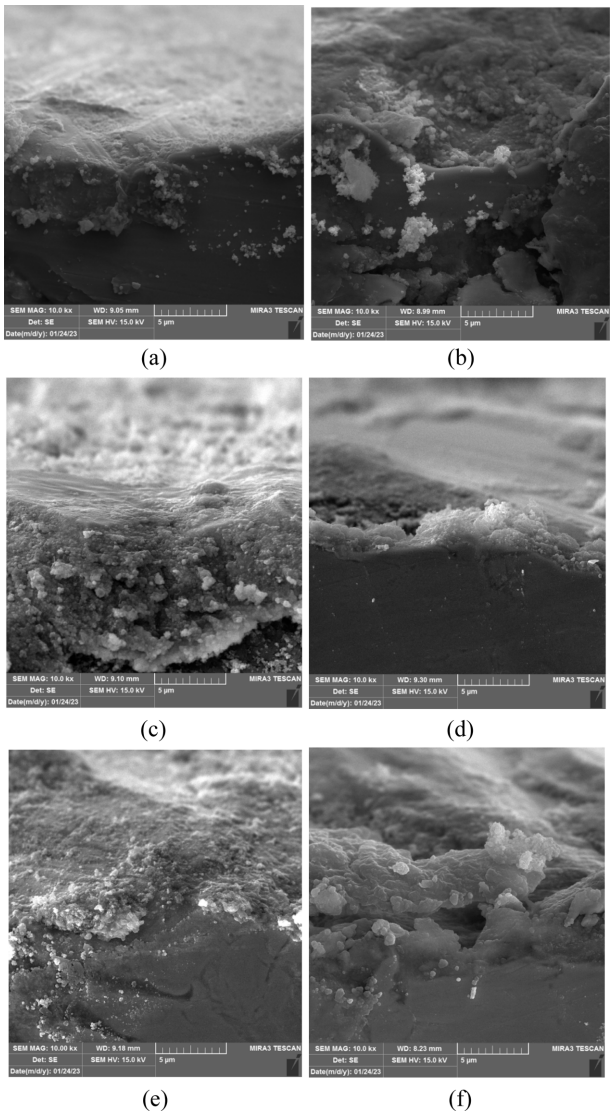

Fig. 1. SEM cross-section for: a) SN2; b) SN3; c) SN4; d) SN5; e) SN6; f) SN7

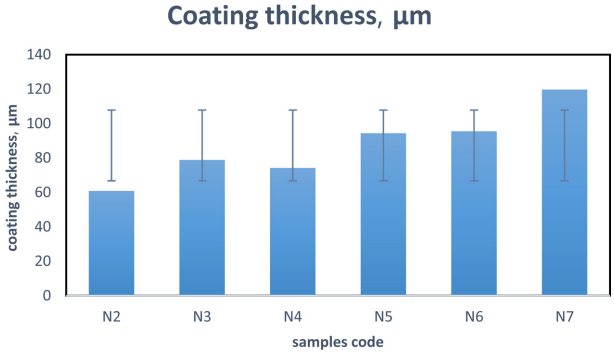

Fig. 2. Coating thickness test result

3.3 Hardness test

The hardness test was performed to assess the impact of Ni-Pb (30 and 60 minutes) and Ni-Pb-TiO_2 (30 and 60 minutes) with titania concentrations of (0.5 and 1.0 wt%) on the hardness magnitudes of the 316 stainless steel, which were initially measured at 245 HV. The experiment aimed to investigate the impact of incorporating ceramic particles of titania (TiO_2) with particle sizes ranging from 10 to 30 µm in varying quantities (0, 0.5, and 1.0) % by weight into a nickel solution. The focus was on evaluating the effect on the hardness properties of the Ni-Pb coating and low-carbon steel specimens. Fig. 4 presents the outcomes of the hardness examination conducted on the steel samples and the Ni-Pb-TiO_2 layers. The disparity in hardness magnitudes observed among the Ni-Pb-TiO_2 layers can be attributed to the variation in the volume fraction of titania present in each

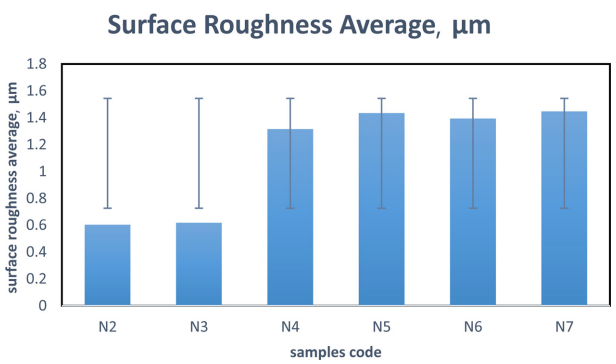

Fig. 3. The surface roughness test result

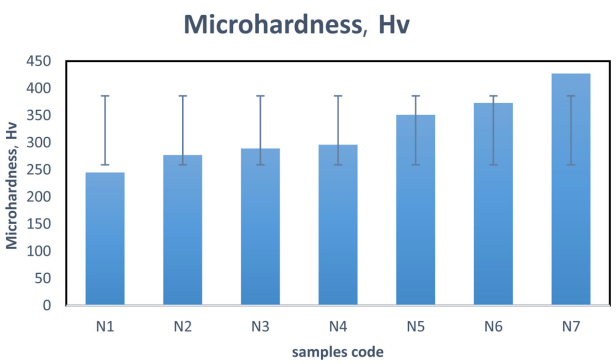

Fig. 4. Hardness improvement rate

layer. The dimensions of the particles influence the hardness of the material and could be mathematically elucidated by the Hall-Petch relationship, as per the established principles [41]:

$$H_V = H_0 + K\sqrt{d} \quad (3)$$

Whereas:

HV : The hardness of material with small-scale particles.

Ho : The hardness of material for multi-scale particles (polycrystalline particle size).

K : Constant magnitude refers to the curve of HV hardness plotted against material type.

d : The diameter of used particles.

The Hall-Petch association is a theoretical framework that elucidates the rationale behind the elevated hardness magnitudes of ultra-fine microstructures, which can reach up to 427 HV, in contrast to their coarser-grained counterparts composed of the same hardened material.

The hardness of the uncoated specimens is enhanced after applying nickel-low phosphor coating, resulting in hardness magnitudes of 277 HV and 289 HV, respectively. Moreover, the augmentation of the added percentage of TiO_2 (0.5 and 1) weight percent can enhance the hardness from 296 HV to 351 HV, 373 HV, and 427 HV. These findings align with the observations made in reference [45]. The detected enhancement can be attributed to the advancements in the morphology of the depth, the distribution, and the increase in the thickness of TiO_2. These improvements are clear in Fig. 4.

Scanning Electron Microscope (SEM) Analysis results.

The SEM images (Fig. 4 A-F) of Ni-Pb-TiO_2 coatings, deposited electrolessly for 30 and 60 minutes with TiO_2 concentrations of 0, 0.5, and 1.0 wt%, demonstrate a gradual increase in TiO_2 content, indicated by the formation of dense, aggregated clusters on the substrate surface. The EDS spectra confirm the incorporation of TiO_2 particles into the Ni-P matrix, showing distinct peaks corresponding to Ti, Ni, and P elements. Quantitative EDS analysis highlights the variation in TiO_2 content, showing a clear relationship with both deposition time and initial TiO_2 concentration. Higher TiO_2 levels promote the formation of compact clusters, increasing coating density. Regions analyzed in the EDS are marked in the micrographs, ensuring alignment between the morphological features and compositional data, providing a coherent understanding of the coating's structural and elemental distribution.

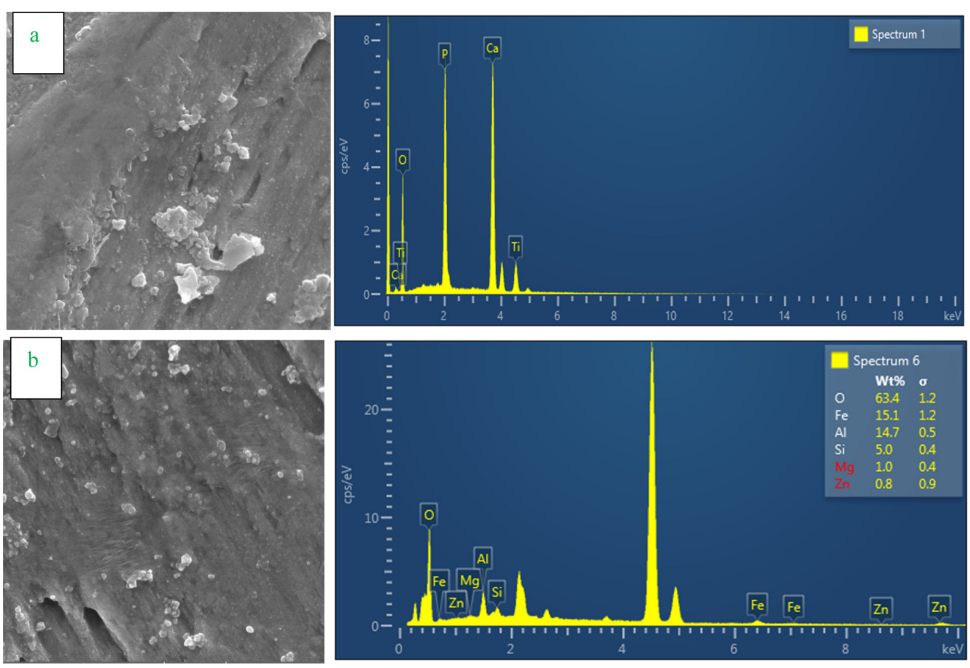

Fig. 5. SEM and EDX images for: a) SN2; b) SN3; c) SN4; d) SN5; e) SN6; f) SN7

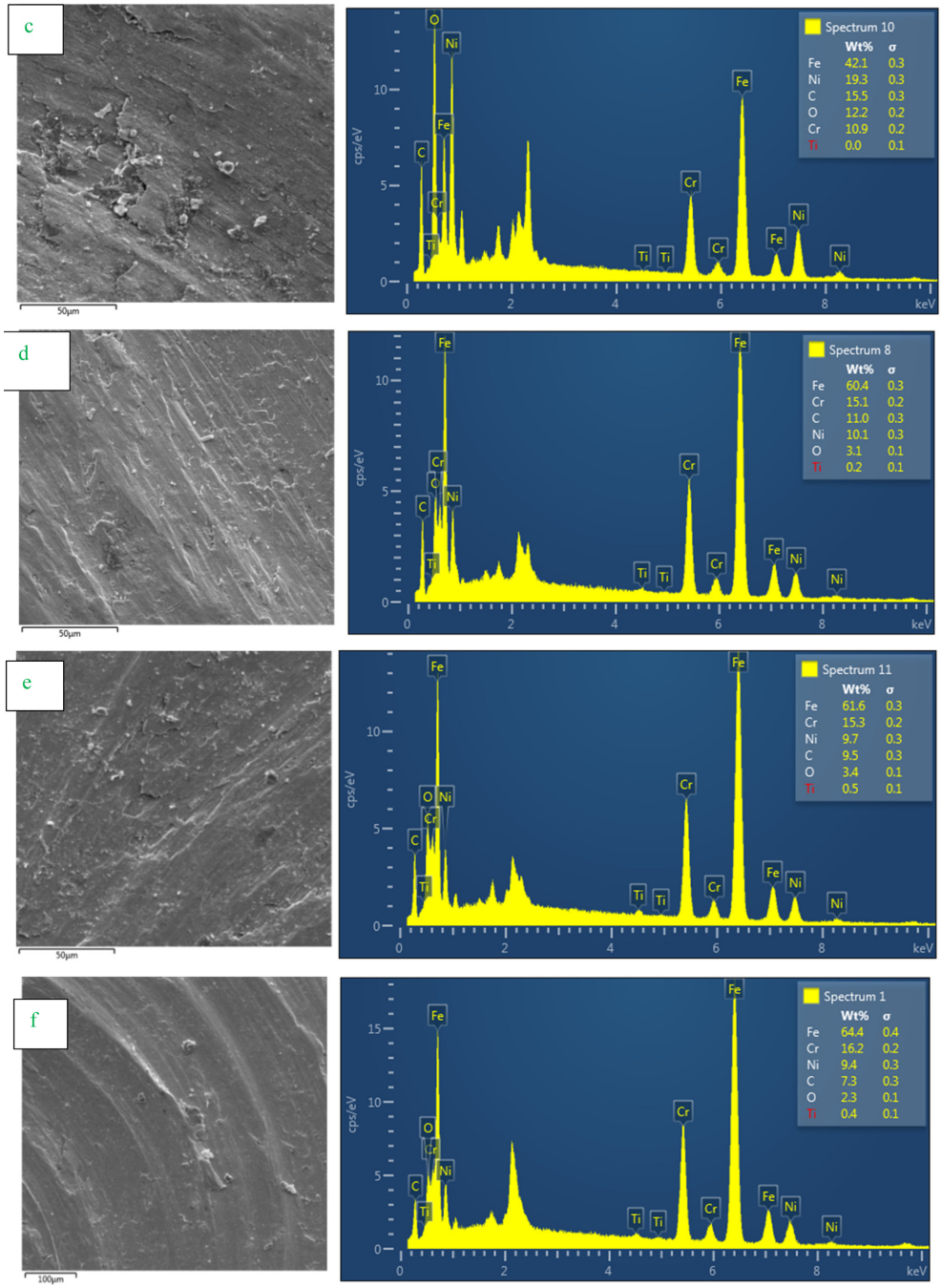

Fig. 5. (Continued) SEM and EDX images for: a) SN2; b) SN3; c) SN4; d) SN5; e) SN6; f) SN7

3.5 Corrosion test

The experimental procedure entailed performing a Potentiodynamic polarization analysis within a 3.5% sodium chloride (NaCl) saline solution, more precisely, a solution simulating seawater conditions. The samples employed in the study were subjected to different surface treatments. These treatments included the application of a coating consisting of nickel-lead (Ni-Pb) for varying durations of 30 and 60 minutes. Additionally, another set of samples was coated with a combination of nickel-lead-titania (Ni-Pb-TiO_2) for the exact durations of 30 and 60 minutes. The titania content in the Ni-Pb-TiO_2 coating varied at 0.5 and 1.0 weight percent. The experimental procedure was conducted at a controlled temperature of 30 degrees centigrade, employing a sample with a surface area of 78.539 cm^2. The corrosion parameters, precisely

Table 3. Corrosion rate (CR) and improvement percent of coated and uncoated samples in 3.5% NaCl solution

Specimens code	icorr. (μA/cm^2)	Ecorr. (mV)	Corrosion Rate (mpy)	Improvement Percentage%
Un-coated specimen	5.27	-446	12.041	-
Ni-Pb 30 min	4.76	-362	10.876	-9.67
Ni-Pb 60 min	3.94	-337	9.002	-25.23
Ni-Pb- 0.5TiO_2, 30 min.	2.98	-354	6.809	-43.45
Ni-Pb-0.5TiO_2, 60 min.	1.74	-279	3.975	-66.98
Ni-Pb-1.0TiO_2, 30 min.	1.93	-293	4.409	-63.38
Ni-Pb-1.0TiO_2, 60 min	1.15	-127	2.627	-78.18

the rate of corrosion, current of corrosion, and potential of corrosion, as acquired from these plots, are displayed in Table 3 and Fig. 6.

To quantify the improvement percentage of the coated samples, Equation (4) has been utilized. A negative value obtained from this equation indicates a reduction in the corrosion rate, signifying enhanced corrosion resistance. Conversely, a positive value represents an increase in the corrosion rate, indicating a decline in the coating's protective performance.

$$\text{Improvement Percentage \%} = \frac{\text{Corrosion Rate for } \textit{coated sample} - \text{Corrosion Rate for } \textit{uncoated sample}}{\text{Corrosion Rate for } \textit{uncoated sample}} \times 100\% \quad (4)$$

The corrosion potential of all the coated specimens exhibits a notable displacement towards the positive direction, indicating a more noble potential. The presence of the coating acts as a protective barrier, effectively mitigating the attack of aggressive ions. Consequently, the corrosion resistance of coated samples is significantly enhanced compared to uncoated 316L stainless steel specimens [45].

The porosity exhibits a reduction upon the introduction of TiO_2 particles. The explanation is substantiated by the empirical evidence indicating that particles substantially impact reducing the corrosion current density and porosity. This phenomenon could be attributed to these minute particles' potential infiltration of the pores. Upon incorporating TiO_2 particles into the Nickel solution, it was detected that the availability of TiO_2 resulted in a substantial reduction in the current density associated with corrosion. This reduction was the most pronounced, as indicated by the lowest recorded magnitude in Table 3 and Fig. 6.

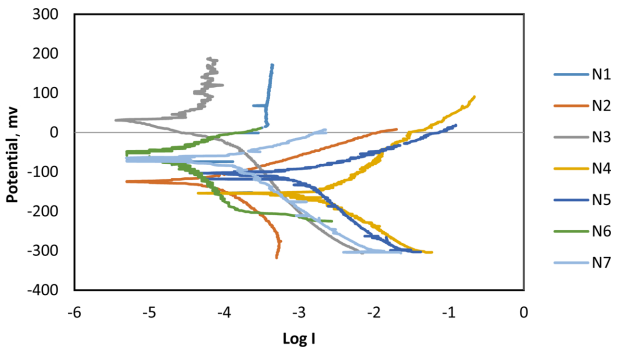

Fig. 6. Liner polyrazation curve of a) SN1; b) SN2; c) SN3; d) SN4; e) SN5; f) SN6 and g) SN7

4. Conclusion

The testing findings of the research have yielded the following conclusions:

1. The analysis revealed that the Ni-Pb and Ni-Pb-TiO_2 composite coatings exhibited complete microparticle coverage, with particle sizes ranging from approximately 10 - 30 μm.

2. The Ni-Pb-TiO_2 composite layer exhibited a structurally stable configuration characterized by a favorable degree of crystallization and surface mechanical bonding, which can be attributed to the effective interaction between TiO_2 and the Ni-Pb matrix.

3. The Vickers hardness magnitudes of the specimens coated with Ni-Pb-TiO_2 at various TiO_2 concentrations (0, 5, and 10) g/L and coating durations (30 and 60) minutes were observed to be (14, 20, 39, 46, 58, and 75)%, respectively.

4. The corrosion rate of the base metal significantly improved with the addition of titania, leading to a 67% increase in the corrosion resistance performance of Ni–Pb–TiO_2 coated SS316.

Future research should emphasize the direct evaluation of corrosion behavior in coated oil pipelines. Comprehensive analyses under simulated operating conditions are essential to assess the coating's efficacy in mitigating internal corrosion. Advanced testing methods and carefully designed evaluation environments should be employed to provide deeper insights into corrosion resistance mechanisms.

References

1. S. Sattar, Y. Alaiwi, N. S. Radhi, Z. Al-khafaji, Numerical Simulation for Effect of Composite Coating (TiO2 + SiO2) Thickness on Steam Turbine Blades Thermal and Stress Distribution, *Academic Journal of Manufacturing Engineering*, **21**, 86 (2023). https://ajme.ro/PDF_AJME_2023_4/L10.pdf
2. S. Sattar, Y. Alaiwi, N. S. Radhi, Z. Al-Khafaji, O. Al-Hashimi, H. Alzahrani, et al. Corrosion reduction in steam turbine blades using nano-composite coating, *Journal of King Saud University-Science*, **35**, 102861 (2023). Doi: https://doi.org/10.1016/j.jksus.2023.102861
3. N. S. Radhi, Z. Al-Khafaji, B. M. Mareai, S. Radhi, A. M. Alsaegh, Reducing Oil Pipes Corrosion By (Zn-Ni) Alloy Coating On Low Carbon Steel Substrate By Sustainable Process, *Journal of Engineering Science and Technology*, **18**, 1624 (2023). https://jestec.taylors.edu.my/Vol%2018%20Issue%203%20June%202023/18_3_19.pdf
4. A. H. Jasim, N. S. Radhi, N. E. Kareem, Z. S. Al-Khafaji, M. Falah, Identify and Investigation Corrosion Behavior of Electroless Composite Coating on Steel Substrate, *Open Engineering*, **13**, ID 472 (2023). Doi: https://doi.org/10.1515/eng-2022-0472
5. E. Mohammed, Z. Al-khafaji, Effect of Surface Treatments by Ultrasonic on NiTi Biomaterials, *Academic Journal of Manufacturing Engineering*, **21**, 77 (2023). Doi: https://ajme.ro/PDF_AJME_2023_3/L11.pdf
6. M. M. Sulaiman, Z. Al-khafaji, Z. N. Shareef, M. Falah, Carbon Capture Based on Chemical Absorption : Process Design and Techno-Economic Assessments, *Engineering Access*, **11**, 57 (2025). Doi: https://doi.org/10.14456/mijet.2025.6
7. G. Haider, H. Arabnejad, S. A. Shirazi, B. S. Mclaury, A mechanistic model for stochastic rebound of solid particles with application to erosion predictions, *Wear*, **376-377**, 615 (2017). Doi: https://doi.org/10.1016/j.wear.2017.02.015
8. M. A. Islam, T. Alam, Z. N. Farhat, A. Mohamed, A. Alfantazi, Effect of microstructure on the erosion behavior of carbon steel, *Wear*, **332-333**, 1080 (2015). Doi: https://doi.org/10.1016/j.wear.2014.12.004
9. M. A. Islam, Z. N. Farhat, Effect of impact angle and velocity on erosion of API X42 pipeline steel under high abrasive feed rate, *Wear*, **311**, 180 (2014). Doi: https://doi.org/10.1016/j.wear.2014.01.005
10. C. Wang, Z. Farhat, G. Jarjoura, M. K. Hassan, A. M. Abdullah, Indentation and erosion behavior of electroless Ni-P coating on pipeline steel, *Wear*, **376-377**, 1630 (2017). Doi: https://doi.org/10.1016/j.wear.2016.12.054
11. X.-H. Yang, W.-L. Zhu, Z. Lin, J.-J. Huo, Aerodynamic evaluation of an internal epoxy coating in nature gas pipeline, *Progress in Organic Coatings*, **54**, 73 (2005). Doi: https://doi.org/10.1016/j.porgcoat.2005.04.001
12. Z. M. Abed Janabi, H. S. Jaber Alsalami, Z. S. Al-Khafaji, S. A. Hussien, Increasing of the corrosion resistance by preparing the trivalent nickel complex, *Egyptian Journal Chemistry*, **65**, 193 (2022). Doi: https://doi.org/10.21608/EJCHEM.2021.100733.4683
13. N. S. Radhi, Z. Al-Khafaji, Investigation biomedical corrosion of implant alloys in physiological environment, *International Journal of Mechanical and Production Engineering Research and Development*, **8**, 247 (2018). Doi: https://doi.org/10.24247/ijmperdaug201827
14. A. Vadde, G. R. Kadambi, Computational analysis of conductive fluid flow with tangential components of magnetic flux density and electric field in metallic and non-metallic circular pipe, *Cogent Engineering*, **10**, 2183797 (2023). Doi: https://doi.org/10.1080/23311916.2023.2183797
15. P. A. Onuh, T. J. Omenma, C. J. Onyishi, C. U. Udeogu, N. C. Nkalu, V. O. Iwuoha, Artisanal refining of crude oil in the Niger Delta: A challenge to clean-up and remediation in Ogoniland, *Local Economy*, **36**, 468 (2021). Doi: https://doi.org/10.1177/02690942211071075
16. A. H. Jasim, N. S. Radhi, N. E. Kareem, Z. S. Al-Khafaji, M. Falah, Identification and investigation of corrosion behavior of electroless composite coating on steel substrate, *Open Engineering*, **13**, 20220472 (2023). Doi: https://doi.org/10.1515/eng-2022-0472
17. S. Brossia, Corrosion Monitoring in Seawater, LaQue's Handbook of Marine Corrosion, 2nd Edition, pp. 633 – 651 (2022). Doi: https://doi.org/10.1002/9781119788867.ch22
18. A. Shokri, M. S. Fard, Corrosion in seawater desalination industry: a critical analysis of impacts and mitigation strategies, *Chemosphere*, **307**, 135640 (2022). Doi: https://doi.org/10.1016/j.chemosphere.2022.135640

19. A. Bahadori, Oil and gas pipelines and piping systems: Design, construction, management, and inspection, 1st Edition, Gulf Professional Publishing (2016). https://shop.elsevier.com/books/oil-and-gas-pipelines-and-piping-systems/bahadori/978-0-12-803777-5
20. A. Bahadori, Cathodic corrosion protection systems: a guide for oil and gas industries, Gulf Professional Publishing (2014). Doi: https://doi.org/10.1016/C2013-0-18442-5
21. P. Ravishankar, Increasing the Oil and Gas Pipeline Resiliency Using Image Processing Algorithms, Lamar University-Beaumont Pro Quest Dissertations & Theses (2023). https://www.proquest.com/openview/f4086ff350fd5a8dbb75ab9b5143f8ef/1?cbl=18750&diss=y&pq-origsite=gscholar
22. A. H. Alamri, Localized corrosion and mitigation approach of steel materials used in oil and gas pipelines–An overview, *Engineering Failure Analysis*, **116**, 104735 (2020). Doi: https://doi.org/10.1016/j.engfailanal.2020.104735
23. A. K. Tewari, Development of green corrosion inhibitors for protection from internal corrosion of buried cross country pipelines (2019). https://dr.ddn.upes.ac.in//xmlui/handle/123456789/2994
24. C. A. Loto, Electroless Nickel Plating – A Review, *Silicon*, **8**, 177 (2016). https://doi.org/10.1007/s12633-015-9367-7
25. R. Karmakar, P. Maji, S. K. Ghosh, A review on the nickel based metal matrix composite coating, *Metals and Materials International*, **27**, 2134 (2021). Doi: https://doi.org/10.1007/s12540-020-00872-w
26. H. Nazari, G. Barati Darband, R. Arefinia, A review on electroless Ni–P nanocomposite coatings: effect of hard, soft, and synergistic nanoparticles, *Journal of Materials Science*, **58**, 4292 (2023). Doi: https://doi.org/10.1007/s10853-023-08281-1
27. V. B. Chintada, R. Koona, M. V. A. Raju Bahubalendruni, State of art review on nickel-based electroless coatings and materials, *Journal of Bio-And Tribo-Corrosion*, **7**, 134 (2021). Doi: https://doi.org/10.1007/s40735-021-00568-7
28. K. H. Krishnan, S. John, K. N. Srinivasan, J. Praveen, M. Ganesan, P. M. Kavimani, An overall aspect of electroless Ni-P depositions—A review article, *Metallurgical and Materials Transactions A*, **37**, 1917 (2006). Doi: https://doi.org/10.1007/s11661-006-0134-7
29. E. M. Fayyad, A. M. Abdullah, M. K. Hassan, A. M. Mohamed, C. Wang, G. Jarjoura, et al. Synthesis, characterization, and application of novel Ni-P-carbon nitride nanocomposites, *Coatings*, **8**, 37 (2018). Doi: https://doi.org/10.3390/coatings8010037
30. M. C. L. de Oliveira, O. V. Correa, B. Ett, I. J. Sayeg, N. B. de Lima, R. A. Antunes, Influence of the tungsten content on surface properties of electroless Ni-WP coatings, *Materials Research*, 21 (2017) Doi: http://dx.doi.org/10.1590/1980-5373-MR-2017-0567
31. F. S. Goettems, J. Z. Ferreira, Wear behaviour of electroless heat treated Ni-P coatings as alternative to electroplated hard chromium deposits, *Materials Research*, **20**, 1300 (2017). Doi: https://doi.org/10.1590/1980-5373-MR-2017-0347
32. S. Roy, P. Sahoo, Optimization of electroless Ni-PW coatings for minimum friction and wear using Grey-Taguchi method, *Journal of Coatings*, **2013**, 1 (2013). Doi: https://doi.org/10.1155/2013/608140
33. M. Cissé, M. Abouchane, T. Anik, K. Himm, R. A. Belakhmima, M. Ebn Touhami, R. Touir, A. Amiar, Corrosion resistance of electroless Ni-Cu-P ternary alloy coatings in acidic and neutral corrosive mediums, *International Journal of Corrosion*, **2010**, 1 (2010). Doi: https://doi.org/10.1155/2010/246908
34. S. Sadreddini, A. Afshar, The effect of heat treatment on properties of Ni–P–SiO_2 nano-composite coating, *Protection of Metals and Physical Chemistry of Surfaces*, **52**, 492 (2016). Doi: https://doi.org/10.1134/S2070205116030254
35. M. Islam, M. R. Azhar, Y. Khalid, R. Khan, H. S. Abdo, M. A. Dar, O. R. Oloyede, T. David, Electroless Ni-P/SiC nanocomposite coatings with small amounts of SiC nanoparticles for superior corrosion resistance and hardness, *Journal of Materials Engineering and Performance*, **24**, 4835 (2015). Doi: https://doi.org/10.1007/s11665-015-1801-x
36. P. Gadhari, P. Sahoo, Study of wear behavior of Ni-P-TiO_2 composite coatings by optimizing coating parameters, *Materials Today Proceedings*, **4**, 1883 (2017). Doi: https://doi.org/10.1016/j.matpr.2017.02.033
37. Z. Antar, M. Masseoud, S. Vesco, M. Barletta, K. Elleuch, Comparative investigation of scratch resistance and tribological performance of Ni–B–TiO_2 composite coatings prepared by conventional and novel processing methods, *Ceramics International*, **47**, 14438 (2021). Doi: https://dx.doi.org/10.1016/j.ceramint.2021.02.023
38. H. Ashassi-Sorkhabi, S. H. Rafizadeh, Effect of coating time and heat treatment on structures and corrosion characteristics of electroless Ni–P alloy deposits, *Surface and Coatings Technology*, **176**, 318 (2004). https://doi.org/

10.1016/s0257-8972(03)00746-1

39. M. A. Shoeib, M. M. Kamel, S. M. Rashwan, O. M. Hafez, Corrosion behavior of electroless Ni–P/TiO_2 nanocomposite coatings, *Surface and Interface Analysis*, **47**, 672 (2015). Doi: https://doi.org/10.1002/sia.5764
40. I. A. Shozib, A. Ahmad, A. M. Abdul-Rani, M. Beheshti, A. A. Aliyu, A review on the corrosion resistance of electroless Ni-P based composite coatings and electrochemical corrosion testing methods, *Corrosion Reviews*, **40**, 1 (2022). Doi: https://doi.org/10.1515/corrrev-2020-0091
41. R. Jensen, Z. Farhat, M. A. Islam, G. Jarjoura, Erosion–Corrosion of Novel Electroless Ni-P-NiTi Composite Coating, *Corrosion and Materials Degradation*, **4**, 120 (2023). Doi: https://doi.org/10.3390/cmd4010008
42. M. Uysal, Electroless codeposition of Ni-P composite coatings: Effects of graphene and TiO 2 on the morphology, corrosion, and tribological properties, *Metallurgical and Materials Transactions A*, **50**, 2331 (2019). Doi: https://doi.org/10.1007/s11661-019-05161-9
43. A. A. Ashtiani, S. Faraji, S. A.Iranagh, A. H. Faraji, The study of electroless Ni–P alloys with different complexing agents on Ck45 steel substrate, *Arabian Journal of Chemistry*, **10**, S1541 (2017). Doi: https://doi.org/10.1016/j.arabjc.2013.05.015
44. ASTM G5-94, Standard reference test method for making potentiostatic and potentiodynamic anodic polarization measurements, ASTM International, **3**, 48 (2004). https://www.scribd.com/document/370560181/ASTM-G5-94-Standard-Practice-pdf
45. N. M. Dawood, N. S. Radhi, Z. S. Al-khafaji, Investigation Corrosion and Wear Behavior of Nickel-Nano Silicon Carbide on Stainless Steel 316L, *Materials Scienc Forum*, **1002**, 33 (2020). Doi: https://doi.org/10.4028/www.scientific.net/MSF.1002.33